# X-ray nanodiffraction of tilted domains in a poled epitaxial $BiFeO_3$ thin film

S. O. Hruszkewycz,[1,a)] C. M. Folkman,[1,2] M. J. Highland,[1] M. V. Holt,[3] S. H. Baek,[2] S. K. Streiffer,[3] P. Baldo,[1] C. B. Eom,[2] and P. H. Fuoss[1]
[1]*Materials Science Division, Argonne National Laboratory, Argonne, Illinois 60439, USA*
[2]*Department of Materials Science and Engineering, University of Wisconsin-Madison, Madison, Wisconsin 53706, USA*
[3]*Center for Nanoscale Materials, Argonne National Laboratory, Argonne, Illinois 60439, USA*

(Received 16 September 2011; accepted 31 October 2011; published online 6 December 2011)

We present measurements of crystallographic domain tilts in a (001) $BiFeO_3$ thin film using focused beam x-ray nanodiffraction. Films were ferroelectrically pre-poled with an electric field orthogonal and parallel to as-grown tilt domain stripes. The tilt domains, associated with higher energy (010) vertical twin walls, displayed different nanostructural responses based on the poling orientation. Specifically, an electric field applied perpendicular to the as-grown domain stripe allowed the domain tilts and associated vertical twin walls to persist. The result demonstrates that thin film ferroelectric devices can be designed to maintain unexpected domain morphologies in working poled environments. © *2011 American Institute of Physics*. [doi:10.1063/1.3665627]

Bismuth ferrite, $BiFeO_3$, has emerged as a model thin film multiferroic material exhibiting antiferromagnetic spin ordering in conjunction with strong ferroelectric polarization ($\sim 95\ \mu C/cm^2$).[1] The (pseudo)rhombohedral spontaneous strain of the $BiFeO_3$ unit cell couples to the polarization and is accommodated by structural twin walls that separate crystallographically distinct domains with coherent interfaces.[2–4] Of particular interest are domain walls that orient vertically in (001) epitaxial rhombohedral thin films. These vertical domain walls (VDWs) produce ferroelastic domains that are tilted away from the surface normal, requiring disclinations at the film-substrate interface to accommodate the tilted local crystallography.[5] Although they have been observed in $BiFeO_3$ heterostructures and other rhombohedrally distorted ferroelectrics, the energy of vertical domain walls is expected to be relatively high,[6] provoking questions about their stability, especially under the influence of external electric fields.

In this work, the stability of VDWs was investigated in an epitaxial $(001)_p$ $BiFeO_3$ thin film grown by radio frequency magnetron sputtering at 690 °C on a $(110)_o$ orthorhombic $TbScO_3$ single crystal substrate[7] (details provided elsewhere[8]). Since the local domain tilting needed to create (100)-type VDWs requires additional coherency defects at the substrate, and because VDWs exhibit a larger surface energy in comparison with slanted (110)-type domain walls,[6] vertical (100) domain walls are expected to be present less frequently in working $BiFeO_3$ ferroelectric devices. This idea is supported in some reports where poled $BiFeO_3$ thin films preferentially exhibit ferroelastic domains with slanted (110)-type twin walls.[9,10] However, we show that by using a specific as-grown domain structure and applied electric field, (100)-type domain walls will persist after poling, highlighting the role of the as-grown nanostructure and external field orientation.

In order to study the response of tilt domains associated with vertical domain walls to applied fields, a 200 nm $BiFeO_3$ film was selected such that the as-grown structure exhibited tilt domains separated by (010) twin walls. This was achieved in part by exploiting the low symmetry $(110)_o$ $TbScO_3$ surface, which biases the as-grown domain population. Instead of the four ferroelastic domain variants predicted for a rhomohedral film grown on a cubic surface (domain types $r_{1-4}$ correspond to rhombohedral elongations along each of the four cubic $\langle 111 \rangle$ directions), two complementary domain variants (e.g., $r_1$ and $r_4$) populated the film.[4,11] These two ferroelastic domain variants can, in turn, exhibit four ferroelectric states $(r_1^+, r_1^-, r_4^+, r_4^-)$. As shown in Figure 1, the as-grown sample exhibited vertical (010) domain twin walls and was comprised of alternating tilted ferroelastic stripe domains. This domain structure allows ferroelectric 109° boundaries between $r_1^-|r_4^+$ or $r_4^+|r_1^-$ at the (010) twin walls as well as 180° boundaries between $r_1^-|r_4^+$ and $r_1^-|r_4^+$ within a single ferroelastic domain. These as-grown ferroelastic and ferroelectric states have been previously observed and verified with x-ray diffraction, transmission electron microscopy, and piezoresponse force microscopy in samples fabricated under the same condition.[9,11]

To investigate the stability of the (010) VDWs in applied electric fields, gold interdigitated electrodes (IDEs) were patterned on the surface of the film in two orientations[12] and in-plane electric fields were applied perpendicular and parallel to the as-grown stripe direction (see Figure 1). The gap between IDE fingers was 6 $\mu$m, the IDE finger width was 9 $\mu$m, and the deposited gold thickness was ~80 nm. Both electrodes were cycled with 1 ms pulses of ±150 V until the film exhibited full saturation ($10^2$ cycles for $E_\perp$ and $10^4$ for $E_{||}$). The hysteresis loops after cycling for each IDE are also shown in Figure 1.

The focused x-ray beam at the Hard X-ray Nanoprobe (operated by the Center for Nanoscale Materials at the Advanced Photon Source) was used to map local diffraction from ferroelastic domain distributions in the as-grown film and in the poled regions. Using an x-ray zone plate optic, 10 keV x-rays were focused to a 40 nm diameter spot that was broadened as needed by defocusing. As shown in Figure 1,

a)Author to whom correspondence should be addressed. Electronic mail: shrus@anl.gov.

 

# Report Documentation Page

*Form Approved*
*OMB No. 0704-0188*



| 1. REPORT DATE | 2. REPORT TYPE | 3. DATES COVERED |
|---|---|---|
| **06 DEC 2011** | | **00-00-2011 to 00-00-2011** |

| 4. TITLE AND SUBTITLE | 5a. CONTRACT NUMBER |
|---|---|
| **X-ray nanodiffraction of tilted domains in a poled epitaxial BiFeO3 thin film** | 5b. GRANT NUMBER |
| | 5c. PROGRAM ELEMENT NUMBER |
| 6. AUTHOR(S) | 5d. PROJECT NUMBER |
| | 5e. TASK NUMBER |
| | 5f. WORK UNIT NUMBER |
| 7. PERFORMING ORGANIZATION NAME(S) AND ADDRESS(ES) **University of Wisconsin-Madison,Department of Materials Science and Engineering,Madison,WI,53706** | 8. PERFORMING ORGANIZATION REPORT NUMBER |
| 9. SPONSORING/MONITORING AGENCY NAME(S) AND ADDRESS(ES) | 10. SPONSOR/MONITOR'S ACRONYM(S) |
| | 11. SPONSOR/MONITOR'S REPORT NUMBER(S) |

12. DISTRIBUTION/AVAILABILITY STATEMENT
**Approved for public release; distribution unlimited**

13. SUPPLEMENTARY NOTES

14. ABSTRACT

15. SUBJECT TERMS

| 16. SECURITY CLASSIFICATION OF: | | | 17. LIMITATION OF ABSTRACT | 18. NUMBER OF PAGES | 19a. NAME OF RESPONSIBLE PERSON |
|---|---|---|---|---|---|
| a. REPORT **unclassified** | b. ABSTRACT **unclassified** | c. THIS PAGE **unclassified** | **Same as Report (SAR)** | **3** | |

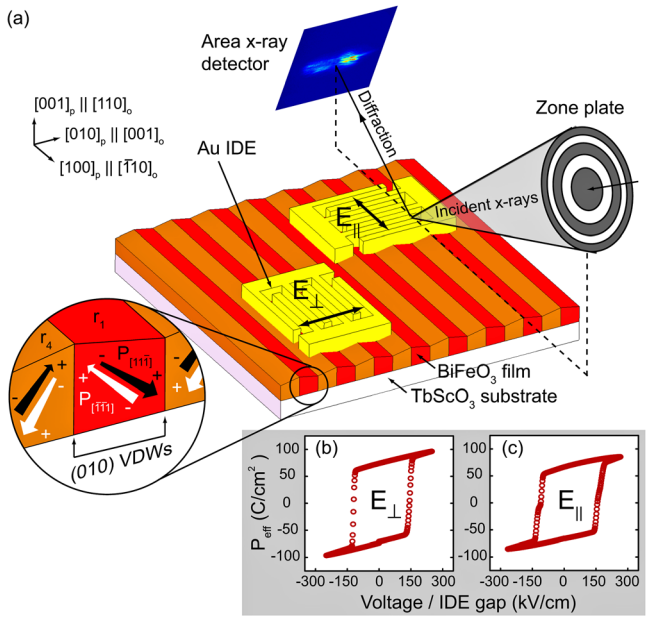


FIG. 1. (Color online) Schematic of the $BiFeO_3$ film, in-plane IDEs, and nanodiffraction experimental setup. Au IDEs were deposited to apply electric fields perpendicular and parallel to the as-grown VDWs. The ferroelectric hysteresis loops from cycling the two IDEs with 1 ms ± 150 V pulses are also shown. Focused beam specular nanodiffraction (shown schematically) was used to probe as-grown and poled regions of the film.

the incoming beam direction was parallel with the as-grown stripe direction and incident on the sample at an angle of 18.25° to satisfy the $(002)_p$ $BiFeO_3$ film diffraction condition. As the beam was scanned over the surface of the film, a CCD area detector was used to record nanodiffraction patterns from which local tilts were extracted. This provides a means to directly measure local *structural* domain interactions and can be a powerful compliment to *polar* domain mapping with piezoresponse force microscopy.[13]

Schematic cross sections are shown in Figure 2 of left tilted (LT), right tilted (RT), and untilted domains (UT) illuminated by a nanofocused beam along with corresponding characteristic specular diffraction patterns. Domains with $(001)_p$ lattice planes tilted away from the surface normal (LT and RT) diffract intensity to either side of the specular $(00L)_p$ reciprocal space vector, whereas domains with untilted $(001)_p$ lattice planes (UT) have no reciprocal space displacement. The film diffraction in this work could be quantified as some combination of these cases. Other domain tilt variants (i.e., into or out of the page in Figure 2) were

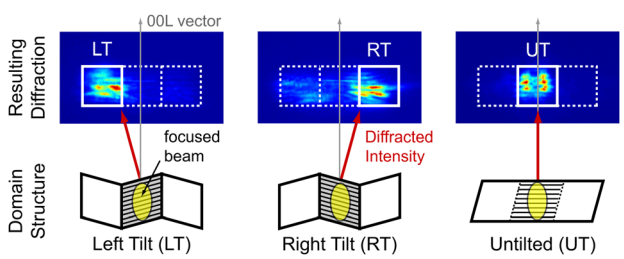


FIG. 2. (Color online) Schematic cross sections are shown (bottom row) of LT, RT, and UT stripe domains that are each illuminated by a nanofocused beam that fits fully inside the domain. The orientation of the illuminated lattice planes determines the local diffracted intensity distribution. The $BiFeO_3$ $(002)_p$ Bragg peak region is coarsely divided into three regions of interest (LT, RT, UT) used to characterize the local domain tilt state.

infrequently observed and are not considered in this analysis. Diffraction from a given volume can, therefore, be separated into RT, LT, and UT components by summing the detector in three regions of interest (shown as white boxes in Figure 2).

Nanodiffraction maps of the two orthogonal IDEs were measured with a defocused beam (250 nm diameter) to first survey the ferroelastic domain tilting in the poled film (Figures 3(b) and 3(d)). The larger beam diameter provided local tilt information from several simultaneously diffracting domains at each scan point to more effectively survey micron-scale areas of the film. These tilt magnitude contrast maps clearly resolve the poled film regions from the as-grown regions covered by the Au electrodes. Scanning electron microscope (SEM) images of equivalent areas are shown for comparison in Figures 3(a) and 3(c), and they reveal a distinct difference in ferroelastic response to poling by in-plane fields $E_{||}$ and $E_\perp$. The as-grown out-of-plane domain tilting persisted after being poled with a perpendicular field and switched to an untilted ferroelastic state after being cycled with a field parallel to the stripe direction. Where $E_\perp$ was applied, the non-uniform electric field at the electrode edge induced local domain reorientations allowing the outline of the electrodes to be observed in diffraction. To understand the local structure in more detail, three characteristic regions, denoted as 1-3 in Figure 3, were chosen that represent three distinct $BiFeO_3$ film conditions: (1) the as-grown film under the Au electrode, $E = 0$, (2) fully poled along the as-grown stripe direction, $E$ along $[010]_p$, and (3) fully poled perpendicular to it, $E$ along $[100]_p$.

The nanoscale tilt domains in these regions were mapped in detail using diffraction from a focused 40 nm diameter beam (Figure 4). At this scale, the characteristic morphology of the as-grown tilt domains is unchanged after poling with a perpendicular applied field (Figures 4(a) and 4(c)), suggesting that ferroelectric alignment can occur in this geometry without removing the (010) twin walls (TWs). These nanodiffraction maps also confirm that the $BiFeO_3$ film is predominantly untitled in regions poled parallel to the as-grown VDWs, consistent with slanted (110)-type twin

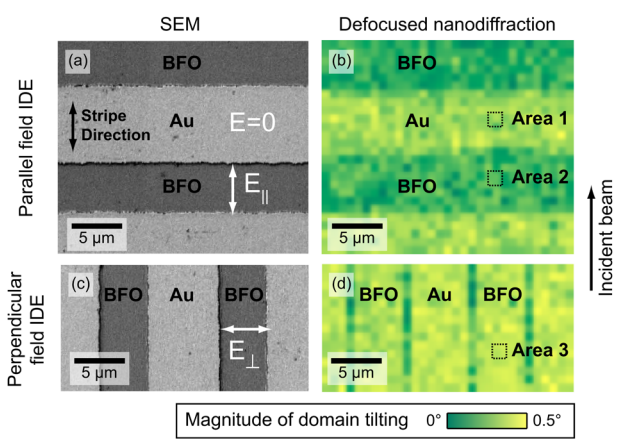


FIG. 3. (Color online) SEM and corresponding x-ray nanodiffractions maps are shown of the IDE regions poled with $E_{||}$ and $E_\perp$ fields. The tilt magnitude maps were made with a ~250 nm diameter defocused x-ray beam and are shown with a color scale given by $(\sum \mathrm{RT} + \sum \mathrm{LT})/\sum \mathrm{UT}$. Areas 1-3 were further studied with a ~40 nm beam.

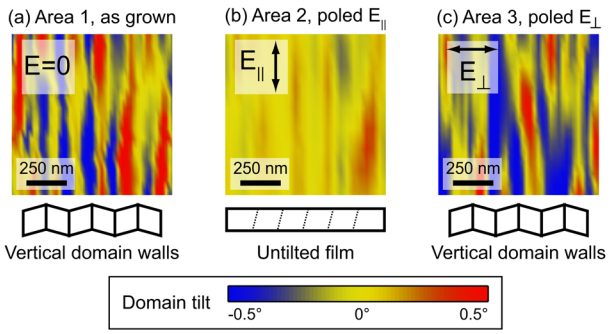


FIG. 4. (Color online) Focused beam nanodiffraction tilt maps of the as-grown and poled $BiFeO_3$ film are shown with contrast given by $(\sum RT - \sum LT)/\sum UT$. The as-grown and poled $E_\perp$ areas exhibit out-of-plane tilting indicative of vertical domain walls, while the $E_{||}$ poled film switched to an untilted state consistent with a monodomain film or with slanted domain walls (dashed lines).

walls (dashed lines in Figure 4(b)) as have been seen experimentally in other studies.[9,10]

Domain walls in ferroelectric thin films interact with electric fields, strain, polarization, and charged defects.[14,15] We found that maintaining a film nanostructure with out-of-plane domain tilts and vertical domain walls required a specific poling direction, a factor which is also correlated to the work needed to pole the film. Poling in the direction normal to the as-grown stripes (maintaining a tilted domain structure) required fewer cycles than were necessary to pole along the stripe direction (crystallographically reorienting the film). This asymmetry ($10^2$ cycles of $E_\perp$ vs. $10^4$ of $E_{||}$) indicates a difference in the energy barriers associated with ferroelectric dipole alignment in the two directions and reflects changes in the ferroelastic domain structure and the associated coherency defects in the $BiFeO_3$ film. Additional contributions to the asymmetric poling behavior may be differences in the mobility of non-ferroelastic (180°) and ferroelastic (109° and 71°) walls in ferroelectric thin films[16,17] as well as preferred polarization rotations of 71° in $BiFeO_3$.[12,15] Future work is needed to isolate these processes and determine their relation to the observation of (010) TWs in poled $BiFeO_3$ thin films.

In summary, focused beam nanodiffraction was used to non-destructively compare domain characteristics in ferroelectrically poled epitaxial $BiFeO_3$ multiferroic films. It was determined that (010)-type twin walls present in the as-grown structure were maintained using a perpendicular electric field orientation. This result demonstrates that applied field orientation contributes to the stabilization of unexpected twin wall formations, having potential impacts on utilization of these nanostructures in functional devices.

This work, including the use of the Center for Nanoscale Materials and the Advanced Photon Source, was supported by the U. S. Department of Energy, Office of Science, Office of Basic Energy Sciences, under Contract No. DE-AC02-06CH11357. The work at UW-Madison was supported by Army Research Office under Grant No. W911NF-10-1-0362 and the National Science Foundation under Grant No. ECCS-0708759.

[1]J. Wang, J. Neaton, H. Zheng, V. Nagarajan, S. Ogale, B. Liu, D. Viehland, V. Vaithyanathan, D. Schlom, U. Waghmare *et al.*, Science **299**, 1719 (2003).
[2]F. Kubel and H. Schmid, Acta Crystallogr. **46**, 698 (1990).
[3]J. Neaton, C. Ederer, U. Waghmare, N. Spaldin, and K. Rabe, Phys Rev. B **71**, 014113 (2005).
[4]S. Streiffer, C. Parker, A. Romanov, M. Lefevre, L. Zhao, J. Speck, W. Pompe, C. Foster, and G. Bai, J. Appl. Phys. **83**, 2742 (1998).
[5]A. Romanov, M. Lefevre, J. Speck, W. Pompe, S. Streiffer, and C. Foster, J. Appl. Phys. **83**, 2754 (1998).
[6]C. Randall, D. Barber, and R. Whatmore, J. Mater. Sci. **22**, 925 (1987).
[7]Here, the subscript *p* denotes a pseudocubic notation for the $BiFeO_3$ rhombohedral unit cell, and the *o* subscript denotes the orthorhombic structure of the scandate substrate.
[8]R. Das, D. Kim, S. Baek, C. Eom, F. Zavaliche, S. Yang, R. Ramesh, Y. Chen, X. Pan, X. Ke *et al.*, Appl. Phys. Lett. **88**, 242904 (2006).
[9]S. Y. Yang, J. Seidel, S. J. Byrnes, P. Shafer, C. H. Yang, M. D. Rossell, P. Yu, Y. H. Chu, J. F. Scott, J. W. Ager *et al.*, Nat. Nanotechnol. **5**, 143 (2010).
[10]L. You, E. Liang, R. Guo, D. Wu, K. Yao, L. Chen, and J. Wang, Appl. Phys. Lett. **97**, 062910 (2010).
[11]C. M. Folkman, S. H. Baek, H. W. Jang, C. B. Eom, C. T. Nelson, X. Q. Pan, Y. L. Li, L. Q. Chen, A. Kumar, V. Gopalan *et al.*, Appl. Phys. Lett. **94**, 251911 (2009).
[12]C. M. Folkman, S. H. Baek, C. T. Nelson, H. W. Jang, T. Tybell, X. Q. Pan, and C. B. Eom, Appl. Phys. Lett. **96**, 052903 (2010).
[13]A. Gruverman, H. Tokumoto, A. Prakash, S. Aggarwal, B. Yang, M. Wuttig, R. Ramesh, O. Auciello, and T. Venkatesan, Appl. Phys. Lett. **71**, 3492 (1997).
[14]T. Rojac, M. Kosec, B. Budic, N. Setter, and D. Damjanovic, J. Appl. Phys. **108**, 074107 (2010).
[15]S. H. Baek, H. W. Jang, C. M. Folkman, Y. L. Li, B. Winchester, J. X. Zhang, Q. He, Y. H. Chu, C. T. Nelson, M. S. Rzchowski *et al.*, Nature Mater **9**, 309 (2010).
[16]F. Xu, S. Trolier-McKinstry, W. Ren, B. Xu, Z. Xie, and K. Hemker, J. Appl. Phys. **89**, 1336 (2001).
[17]M. Kohli, P. Muralt, and N. Setter, Appl. Phys. Lett. **72**, 3217 (1998).